Published in final edited form as:
Dev Neurobiol. 2011 September ; 71(9): 747–758. doi:10.1002/dneu.20907.

The Actin Nucleating Arp2/3 Complex Contributes to the Formation of Axonal Filopodia and Branches Through the Regulation of Actin Patch Precursors to Filopodia

Mirela Spillane[1], **Andrea Ketschek**[1], **Steven L. Jones**[1], **Farida Korobova**[2], **Bonnie Marsick**[3], **Lorene Lanier**[3], **Tatyana Svitkina**[2], and **Gianluca Gallo**[1,*]

[1]Drexel University College of Medicine, Department of Neurobiology and Anatomy, 2900 Queen Lane, Philadelphia PA 19129

[2]University of Pennsylvania, Department of Biology, 415 S. University Avenue, Philadelphia, PA 19104

[3]University of Minnesota, Department of Neuroscience, 321 Church Street, Minneapolis, MN 55455

Abstract

The emergence of axonal filopodia is the first step in the formation of axon collateral branches. *In vitro*, axonal filopodia emerge from precursor cytoskeletal structures termed actin patches. However, nothing is known about the cytoskeletal dynamics of the axon leading to the formation of filopodia in the relevant tissue environment. In this study we investigated the role of the actin nucleating Arp2/3 complex in the formation of sensory axon actin patches, filopodia and branches. By combining *in ovo* chicken embryo electroporation mediated gene delivery with a novel acute *ex vivo* spinal cord preparation, we demonstrate that actin patches form along sensory axons and give rise to filopodia *in situ*. Inhibition of Arp2/3 complex function *in vitro* and *in vivo* decreases the number of axonal filopodia. *In vitro*, Arp2/3 complex subunits and upstream regulators localize to actin patches. Analysis of the organization of actin filaments in actin patches using platinum replica electron microscopy reveals that patches consist of networks of actin filaments, and filaments in axonal filopodia exhibit an organization consistent with the Arp2/3-based convergent elongation mechanism. Nerve growth factor (NGF) promotes formation of axonal filopodia and branches through phosphoinositide 3-kinase (PI3K). Inhibition of the Arp2/3 complex impairs NGF/PI3K-induced formation of axonal actin patches, filopodia, and the formation of collateral branches. Collectively, these data reveal that the Arp2/3 complex contributes to the formation of axon collateral branches through its involvement in the formation of actin patches leading to the emergence of axonal filopodia.

Keywords

WAVE1; cortactin; Arp2; spinal cord; growth cone

INTRODUCTION

The function of the nervous system is dependent on complex networks of synapses between neurons. In order to establish connections with multiple neurons axons give rise to collateral

*corresponding author. Ph: 215-991-8288, Fax: 215-843-0980; GGallo@drexelmed.edu.

Conflict of Interest: none

branches (Cohen-Cory et al., 2010; Gibson and Ma, 2011). The extension of axonal filopodia is the first step in the formation of axon collateral branches (Bastmeyer and O'Leary, 1996; Portera-Cailliau et al., 2005; reviewed in Gallo, 2011) and presynaptic structures (Gan, 2003). Axons give rise to many transient filopodia but only a few filopodia mature into collateral branches (Gallo, 2011). The formation of axonal filopodia and their maturation into collateral branches is regulated by extracellular signals (Gibson and Ma, 2011). *In vitro*, axonal filopodia emerge from precursor axonal accumulations of actin filaments termed actin patches in a variety of neuron types (Loudon et al., 2006; Gallo, 2006; Orlova et al., 2007; Korobova and Svitkina, 2008; Mingorance-Le Meur, O'Connor, 2009; Ketschek and Gallo, 2010). Actin patches arise spontaneously along the axon and are transient structures. Similar to the maturation of only a subset of filopodia into branches, only a fraction of actin patches give rise to axonal filopodia. Thus, the formation of a collateral branch is the culmination of the formation of many actin patches, some of which give rise to filopodia, and in turn the maturation of a subset of filopodia into branches. Although a variety of molecules have been implicated in the formation of axonal filopodia and branches, little is known about their specific roles in the underlying cytoskeletal mechanisms (Gibson and Ma, 2011; Gallo, 2011).

Phosphoinositide 3-kinase (PI3K) signaling is a major regulator of axonal morphology (Cosker and Eickholt, 2007). PI3K is a lipid kinase that phosphorylates phosphatidylinositol (4,5)-bisphosphate (PIP2) resulting in the generation of phosphatidylinositol (3,4,5)-trisphosphate (PIP3). PIP3 in turn recruits protein kinases and other proteins to the membrane resulting in the activation of signaling mechanisms. *In vivo* depletion of PTEN, the phosphatase that antagonizes the activity of PI3K, promotes axon branch formation through a poorly understood mechanism (Kwon et al., 2006; Drinjakovic et al., 2010). Nerve growth factor (NGF) induces axon branching *in vivo* and *in vitro* (Gallo and Letourneau, 1998; Patel et al., 2000; Petruska and Mendell, 2004) and promotes the formation of axonal filopodia and branches through a PI3K-dependent mechanism (Gallo and Letourneau, 1998; Ketschek and Gallo, 2010). PI3K activity gives rise to localized microdomains of PIP3 along the axon that determine the spatio-temporal development of axonal actin patches and filopodia (Ketschek and Gallo, 2010). Importantly, NGF-PI3K signaling increases the rate of formation of actin patches without affecting the probability that an individual patch will give rise to a filopodium (Ketschek and Gallo, 2010; Ketschek et al., 2011). Thus, the rate of actin patch formation is a major regulatory point in the NGF-induced increase in the formation of axonal filopodia and ultimately branches. Although the initiation of actin patches is a critical point in the regulation of axonal filopodia, the underlying cytoskeletal mechanisms remain elusive.

Unlike the highly dynamic growth cone, the axon shaft exhibits low levels of actin filaments and little protrusive activity (Letourneau, 2009). The mechanisms that locally regulate the axonal cytoskeleton underlying the initiation of filopodia are minimally understood. The first step in the formation of actin-based structures is the nucleation of actin filaments from monomers. Actin filaments can be nucleated de novo as single filaments by nucleation factors or from the sides of existing filaments by the Arp2/3 complex, giving rise to branched filament arrays. A role for both types of actin nucleation mechanisms in the formation of filopodia has been shown in non-neuronal and neuronal cells (Mattila and Lappalainen, 2008; Faix et al., 2009; Lundquist, 2009). In this report we address the role of the actin nucleating Arp2/3 complex in the formation of axonal actin patches, filopodia and collateral branches. We demonstrate that actin patches serve as precursors to the formation of axonal filopodia along sensory axons in the developing spinal cord and that the Arp2/3 complex contributes to the formation of axonal actin patches and in turn filopodia and branches.

MATERIALS AND METHODS

Culturing, transfection and immunocytochemistry

Culturing, nucleofection (Amaxa), and live imaging was performed as described in Ketschek and Gallo (2010). Briefly, dorsal root ganglia were dissected from embryonic day 7 chicken embryos and dissociated prior to transfection using Nucleofection based electroporation using chicken neuron specific transfection reagents (Amaxa Inc). 10 μg of plasmid were used routinely for transfections. Dissociated cells were cultured overnight on laminin (25 μg/mL; Invitrogen) coated coverslips or video imaging chambers (same chambers as shown in Fig 1B for spinal cord *ex vivo* imaging). GFP-CA and GFP-p21 constructs were used as in Strasser et al (2004), and RFP-cortactin as described in Mingorance-Le Meur and O'Connor (2009), additional plasmids were described in Ketschek and Gallo (2010). Treatment with NGF (30 min, 40 ng/mL) and PI3Kpep (1 hr, 50 μg/mL) or the control PI3KpepAla peptide was performed as previously described (Ketschek and Gallo, 2010). For immunocytochemistry using p34 (Upstate Biotechnology: 1:200) and Arp3 (Santa Cruz Biotechnology: 1:100) antibodies cultures were fixed and processed as described in Korobova and Svitkina (2008). For Arp2 staining (ECM Biosciences; 1:100) cultures were fixed in 8% paraformaldehyde in PHEM buffer containing 5% sucrose, 5 μM jasplakinolide (Calbiochem), 10 μM taxol (Sigma) and 0.2% NP-40. WAVE1 (ECM Biosciences; 1:50) and cortactin (ABcam, ab11065; 1:250) were detected in cultures fixed with 0.25% glutaraldehyde or 8% paraformaldehyde with 5% sucrose, respectively. All glutaraldehyde fixed cultures were treated with 2 mg/mL sodium borohydride (15 min). All cultures were blocked for 30 min in 10% goat serum containing 0.1% triton X-100 (GST), stained with primary antibodies for 1 hr in GST, followed by washing and staining with secondary antibodies in GST and phalloidin (Molecular Probes).

Filopodia were defined as either phalloidin stained axonal finger-like protrusions or axonal protrusion less than 10 μm in GFP expressing neurons, *in vitro*. Based on our previous characterization of collateral formation by sensory axons *in vitro*, in GFP expressing neurons branches were defined as protrusion greater than 10 μm in length (Gallo and Letourneau, 1999). The dynamics of axonal actin patches were determined as previously described in Ketschek and Gallo (2010).

Platinum replica electron microscopy (PREM)

Dissociated neuron cultures were simultaneously fixed and extracted using 0.25% glutaraldehyde and 0.5% Triton X-100 in PEM buffer containing 4 μM jasplakinolide (Calbiochem) and 10 μM taxol (Sigma) for 5 min and postfixed with 2% glutaraldehyde in 0.1 M sodium cacodylate (pH 7.3). Subsequent sample preparation was performed as previously described (Korobova and Svitkina, 2008), Samples were imaged using a JEM 1011 transmission electron microscope (JEOL USA, Peabody, MA) operated at 100 kV. Images were captured by ORIUS 835 10W CCD camera (Gatan, Warrendale, PA) and presented in inverted contrast.

In ovo electroporation and *ex vivo* imaging

Chicken embryos were electroporated in ovo at embryonic day (ED) 3 using a CUY-21SC electroporator (Nepa Gene) equipped with 3 mm L-shaped gold tip electrodes (Harvard Apparatus) using five 50 ms 50V pulses at a rate of 1 pulse per second. Plasmids were injected (0.1–0.15 μg/μL PBS with 0.01% fast green) into the lumen of the neural tube and electrodes placed at the level of the lumbosacral enlargement. In each embryo, 3–5 lumbosacral DRG and cells in the neural tube were transfected unilaterally (Figure 1A). At ED 7 the embryos were extracted from the eggs and the entire spinal cord caudal to the first thoracic segment was dissected out. The cord was next separated into two halves by severing

the floor and roof plates and immediately placed in the well of a video-imaging dish (as in Ketschek and Gallo, 2010) containing 20 μL of culturing medium (Figure 1B). The well of the video dish was then enclosed by placing a glass coverslip on top of the well in the dish and sealed to the dish by a ring of medium between the glass and dish surface. The assembled video-dish was immediately used for imaging experiments and discarded after 1 hr. During this period we have used 20× imaging to measure the rate of GFP expressing DRG axon extension in the cord and found it to remain constant (not shown), and the general morphology of growth cones did not vary, indicating that the cord is viable for at least 1 hr. Imaging was performed as for the *in vitro* experiments using a Zeiss 200M inverted microscope equipped with an Orca ER CCD camera (Hamamatsu). For imaging we used Zeiss Pan-Neofluar 100× and 20× objectives with 1.3 and 0.5 numerical apertures, respectively.

Statistical analysis

Analysis of data sets was performed as described in Ketschek and Gallo (2010) using Instat software (GraphPad Inc).

RESULTS

Axonal actin patches give rise to filopodia in the spinal cord

The formation of filopodia from axonal actin patches has only been demonstrated *in vitro*. We sought to determine whether sensory axons form actin patches in the spinal cord. In order to image axons in the spinal cord we delivered plasmid vectors encoding fluorescently tagged proteins to the developing lumbosacral dorsal root ganglia (DRG) of chicken embryos using in ovo electroporation (Figure 1A). We analyzed ED 7 embryos, when sensory axons begin to form collateral branches *in vivo* (Davis et al., 1989). The spinal cord was dissected from the embryos and immediately imaged to detect fluorescently tagged axons (Figure 1B). In the lumbosacral region the DRG were transfected and there were also transfected cells in the spinal cord, likely reflective of glia and inter-neurons (not shown). However, in the segments of the cord rostral and caudal to the electroporated region, only transfected DRG axons were present in the dorsal funniculi, as expected based on the anatomy of the sensory system (Figure 1C). We focused the imaging analysis on the caudal portion of the cord because the tissue is thinner relative to rostral regions. Using conventional epifluorescence microscopy we were able to image GFP-labeled axons, axonal filopodia (Figure 1D), branches (Figure 1E) and growth cones (Figure 1F) at 100× magnification.

To monitor the dynamics of the axonal actin cytoskeleton in the living spinal cord, embryos were electroporated *in ovo* with GFP-actin and RFP. We imaged a total of 10 cotransfected axons at 100× from three spinal cord preparations each for 5 minute periods at 6 seconds interframe intervals. The summed length of the axons imaged was 380 micrometers (mean length/axon=35±6 μm) and we detected a total of 52 patches forming. The initiation and elaboration of patches was wholly similar to that previously described for DRG axons growing *in vitro* (Figure 1G). Furthermore, as *in vitro*, actin patches served as precursors to the formation of axonal filopodia (Figure 1G). In regions of patch formation the actin signal increased to a mean maximum of 76±5% from the baseline. The RFP signal, representative of potential volumetric changes, increased only 6±7% ($p<0.0001$, compared to the increase in actin) demonstrating that as *in vitro* the accumulation of actin is independent of volumetric changes (Ketschek and Gallo, 2010). Dividing the total number of patches formed by the total length of axon measured yields a frequency of 2.08 patches/20 μm/5 min.

In order to compare the dynamics of actin patches in the spinal cord to those observed *in vitro* we used age matched ED7 cultured neurons in the presence of NGF. NGF was included in the experimental design because axons sampled *in situ* in the spinal cord are in the early stage of collateral branch formation (Mendelson et al., 1992), a process which *in vivo* is largely driven by branch-inducing factors (reviewed in Gibson and Ma, 2011). Thus, NGF was used *in vitro* to mimic the expected branch-promoting environment of the spinal cord. In the spinal cord we sampled from axons between approximately 500–1500 μm from the cell body, and we thus sampled the middle segments of axons *in vitro* ranging between 700–1300 μm in length A summary of the comparison of in vitro axons to axons in the spinal cord is presented in Table 1. The rate of actin patch formation sampled *in vitro* is 2.04±0.36 patches/20 μm/5 min (mean±SEM, n=9 axons, 71 patches). Thus, based on sampling from equivalent segments of the axons in an *in vitro* environment designed to best match the expected *in vivo* environment, the rate of actin patch formation is not distinguishable between *in vitro* and in the *ex vivo* spinal cord.

Analysis of the probability of the emergence of a filopodium from a patch revealed that 17% of patches gave rise to filopodia in axons growing within the spinal cord, similar to the 15% observed *in vitro* for equivalent segments of DRG axons (n=71 patches). The mean lifespan of actin patches in the cord was 41.4±1.8 sec compared to 48.0±4.6 sec *in vitro* ($p>0.16$). In order to determine if patches developed to different sizes *in vitro* relative to in the spinal cord, we sampled the timelapse sequences every 40 seconds and determined the area of patches. The size of patches was not different between the axons *in vitro* or in the spinal cord (Table 1). These observations reveal for the first time that axonal actin patches are formed by DRG axons in the context of the environment of the spinal cord, where these axons form branches, and that as *in vitro* patches serve as precursors to the formation of filopodia. However, measurement of the length of filopodia indicate that filopodia in the spinal cord attain shorter lengths than in vitro (2.9 microns median, n=146, in the spinal cord and 3.6 microns median in vitro, n=73; Mann-Whitney test $p<0.01$).

We have previously reported that the rate of actin patch formation exhibits a distal (higher)-proximal(lower) gradient in the distal 40 μm of ED7 axons *in vitro* (Ketschek and Gallo, 2010). The current data analyzing actin patches hundreds of microns from the growth cone indicates a further decrease of approximately 60% relative to the axon segment 20–40 μm from the growth cone. Interestingly, the lifespan of patches exhibits an opposite proximal(higher)-distal(lower) gradient. In the distal 20 μm of axons the mean lifespan of patches is approximately 20 seconds compared to 48 seconds in the middle of the axons ($p<0.001$). These data thus indicate the presence of opposite gradients of the mechanisms that initiate actin patches and control the lifespans of patches along the axon, respectively. However, the frequency of emergence of filopodia is largely conserved throughout the axon (23% in the distal 20 μm of the axon and 15% in the middle segments; Fischer's Exact test, $p>0.15$).

The Arp2/3 complex localizes to axonal actin patches

The Arp2/3 complex is composed of seven proteins (Arp2, Arp3, p16, p20, p21, p34, p40) and is regulated by upstream factors including cortactin and WAVE1. Using immunocytochemistry we detected the Arp2, Arp3, and p34 subunits and both cortactin and WAVE1 in axonal actin patches *in vitro* in the presence and absence of NGF alike (Figure 2A). Furthermore, dual channel time-lapse imaging of GFP-p21 and mCherry-actin, to simultaneously track actin patches, determined that the p21 subunit is recruited to 89% of patches early on in patch development and persists for the lifespan of the patches (9 axons, 84 patches; Figure 2B). Imaging RFP-cortactin and eYFP-actin revealed that cortactin similarly targets to 92% of actin patches (8 axons, 64 patches; Figure 2C). The areas of actin patches detected in fixed axons vary from patch to patch. This variation is likely due to

individual patches being fixed at different times during their lifespan (see Supplementary Material).

Cytoskeletal organization of axonal actin filaments

To determine the organization of actin filaments in the axon we used platinum replica electron microscopy (PREM), a technique that provides single filament resolution (Svitkina, 2009). Consistent with phalloidin staining patterns, actin filaments in the axon were sparse and often detectable as individual filaments among abundant microtubules (Figure 3A). The most prominent accumulations of actin filaments in the axon were lateral patches of the actin filament network associated with the microtubule array (Figure 3B,C). Based on their location, size and paucity of other actin filament-enriched structures as detected by phalloidin staining, the accumulations of actin filaments detected by PREM are likely reflective of actin patches detected by phalloidin or live imaging. We however cannot exclude that some of the detected structures may not be actin patches as observed through phalloidin or live imaging of fluorescently tagged actin. Although the density and three-dimensionality of the actin network within patches often precluded full analysis of the network organization, at the edges of patches we were able to detect branched filaments with an average angle of 68±1.5 degrees (n=38) (Figure 3D) that is characteristic for Arp2/3 complex-mediated nucleation (Pollard et al., 2000). Some actin patches contained a bundle of long actin filaments extending perpendicular to the axon shaft, a characteristic feature of actin filament organization in filopodial shafts. These bundles emerged from the meshwork in a pattern consistent with the convergent elongation model proposed for the formation of filopodia from Arp2/3-generated filaments (Figure 3E; Svitkina et al., 2003).

Inhibition of the Arp2/3 complex impairs the formation of axon branches, actin patches and filopodia

To functionally address the role of the Arp2/3 complex we expressed the inhibitory peptide CA in cultured sensory neurons (Strasser et al., 2004). The Arp2/3 complex has endogenously low activity and the CA construct acts as a competitive antagonist to the binding of upstream activators. Expression of GFP-CA relative to GFP decreased the numbers of axon collateral branches formed by cultured ED 7 neurons raised in the presence of the branch inducing factor NGF (Figure 4A) without altering the length of branches that formed (Figure 4A), and decreased the number of axonal filopodia by 58% ($p<0.05$).

Spontaneous formation of actin patches in ED 7 sensory neurons growing on laminin in the absence of NGF is dependent on integrin and PI3K signaling, and NGF treatment promotes formation of axonal filopodia by increasing the rate of actin patch initiation in a manner dependent on PI3K activity (Ketschek and Gallo, 2010). To analyze the role of the Arp2/3 complex in actin patch formation we determined the effects of GFP-CA expression on the rate of mCherry-actin patch formation before and after treatment with NGF. Expression of GFP-CA decreased the rate of patch formation in the absence of NGF and blocked the NGF-induced increase in the rate of patch formation (Figure 4B). Similarly, treatment with a pharmacological inhibitor of Arp2/3 (CK-869; Nolen et al., 2009) decreased actin patch formation in the absence or presence of NGF (Figure 4C). CK-869 was used at 50 μM, the concentration that maximally decreased formation of lamellipodia in cultured chicken kidney cells (Silver et al., 2004; data not shown), consistent with its characterization (Nolen et al., 2009).

NGF treatment does not affect the proportion of actin patches that give rise to filopodia (Ketschek and Gallo, 2010). Expression of GFP-CA did not affect the proportion of patches that gave rise to filopodia either before ($p>0.29$, Fischer's exact test) or after NGF treatment ($p>0.33$), compared to GFP expressing neurons. NGF treatment did not affect the duration

(seconds) of newly formed filopodia in control GFP expressing neurons ($p>0.7$, Welch t-test). GFP-CA also had no effect on the duration of filopodia that formed before ($p>0.72$) or after NGF treatment ($p>0.34$), compared to GFP controls. The maximal length attained by filopodia was also not affected by expression of GFP-CA either before ($p>0.63$) or after NGF treatment ($p>0.7$). Collectively these data indicate that the Arp2/3 complex mediates formation of axonal actin patches but the mechanism that determines the emergence of filopodia from patches and their subsequent elongation is independent of Arp2/3.

The formation of NGF-dependent and independent axonal actin patches and filopodia is driven by axonal microdomains of PI3K-induced PIP3 accumulation (Ketschek and Gallo, 2010). NGF promotes the formation of axonal PIP3 microdomains, and in turn actin patches and filopodia, but NGF has no effect on the total intensity of Factin as detected by phalloidin staining in patches ($p=0.96$, $n=54$ and 64 for pre and post NGF treatment) and the duration/lifespan of actin patches (Ketschek and Gallo, 2010). Direct activation of PI3K using a cell permeable phospho-peptide (PI3Kpep) in the absence of NGF increases formation of PIP3 microdomains and the accompanying actin patches (Ketschek and Gallo, 2010; Figure 4D). PI3Kpep activates PI3K by mimicking the activated tyrosine phosphorylated PDGF receptor (Williams and Doherty, 1999) and PI3KpepAla is an inactive control as the phospho-tyrosine residue is replaced with alanine (Ketschek and Gallo, 2010), both peptides are rendered permeable by an in-tandem antennapedia peptide sequence. Expression of GFP-CA blocked the increase in the rate of formation of axonal actin patches induced by PI3Kpep (Figure 4D). Similarly, co-treatment with CK-869 prevented the increase in axonal filopodia number induced by PI3Kpep ($p<0.001$; $n>49$ axons/group, 1 hr treatments) while decreasing the number along control PI3KpepAla treated axons by 40% ($p<0.04$).

Using the acute *ex vivo* spinal cord preparation (Figure 1) we determined that in ovo expression of GFP-CA decreases the numbers of filopodia along axons extending in the spinal cord. Embryos were transfected with GFP or GFP-CA and spinal cord preparations were imaged as previously described at ED 7. We measured the mean number of filopodia per unit length of distal axon (0 to 40 μm behind the growth cone, as *in vitro*). Data were obtained from a region of the cord up to 2 mm caudal to the transfected DRG in 2 and 4 embryos transfected with GFP and GFP-CA, respectively. GFP and GFP-CA expressing axons exhibited 5.6±0.5 ($n=40$) and 2.8±0.4 filopodia ($n=38$), respectively ($p<0.0001$, Welch t-test) (Figure 4E). As noted previously, filopodial lengths in the cord exhibited a non-normal distribution with a median length of 2.9 microns ($n=146$). Analysis of the distribution of the lengths of axonal protrusions greater than twice the median length of the GFP group (>6 microns), which are likely reflective of nascent branches, reveals that GFP-CA expression ($n=143$) decreases the proportion of these longer protrusions by 41% relative to GFP ($n=115$) ($p<0.05$; Fischer's exact test).

DISCUSSION

The formation of axon collateral branches is poorly understood. The first step in the development of a collateral branch is the initiation of actin based protrusive activity along the otherwise quiescent axon shaft (Gallo, 2011). To understand the mechanisms of axon branching it is necessary to link specific signaling pathways to discrete cytoskeletal events. This study determines the involvement of the Arp2/3 complex in one of the earliest steps in collateral branch formation, the initiation of the axonal actin patches that serve as precursors to the emergence of axonal filopodia. The demonstration that inhibition of the Arp2/3 complex impairs the formation of neuronal filopodia is consistent with inhibition of growth cone filopodia formation after knockdown of Arp2/3 complex subunits (Korobova and Svitkina, 2008) and the role of Arp2/3 in the formation of growth cone filopodia *in vivo* in C elegans (Norris et al., 2009). The impairment of sensory axon collateral branches without

affecting the length of branches that form is consistent with a prior report using hippocampal neurons (Strasser et al., 2004). Collectively, the data indicate that the Arp2/3 complex contributes to the formation of axonal actin patches that serve as precursors to the formation of axonal filopodia and in turn branches. However, the rate of emergence of filopodia from patches and the subsequent duration and extension of filopodia is independently regulated.

In this paper we demonstrate that in embryonic sensory neurons Arp2/3 complex subunits and upstream regulators target to actin patches and that inhibition of Arp2/3 activation *in vitro* and *in vivo* through expression of the CA peptide decreases the formation of filopodia. However, we note that decreases in filopodia along the distal 100 μm of axons were not observed in cultured hippocampal neurons expressing the CA peptide and expression of CA did not impair the increase in filopodia number induced by netrin (Strasser et a., 2004). The discrepancies between these studies likely reflect a difference in neuronal cell types, culturing conditions or a difference between NGF and netrin signaling mechanisms. Furthermore, the Arp2/3 complex has been shown to be required for formation of filopodia in some but not all non-neuronal cell types (Mattila and Lappalainen, 2008; Faix et al., 2009; Lundquist, 2009). Further analysis will be required to address the differences in the mechanisms of the formation and regulation of axonal filopodia in different neuron types and by different filopodia/branch-inducing signals. Additionally, the formation of collateral branches from filopodia formed de novo from the otherwise quiescent axon shaft has been demonstrated in multiple neuron systems *in vivo* and *in vitro* (reviewed in Gallo, 2011). However, cortical axons extending across the corpus callosum form collateral branches through a mechanism involving the determination of the site of collateral formation by the transient stalling of the growth cone which leaves behind a domain of the axon exhibiting protrusive activity (Halloran and Kalil, 1994; Kalil et al., 2000). It remains to be determined if a similar PI3K-Arp2/3 dependent mechanism is operative during the collateral branching of callosal cortical neurons.

Actin patches serve as precursors to the formation of dendritic filopodia *in vivo* in Drosophila (Andersen et al, 2005). Using a novel acute *ex vivo* spinal cord preparation we demonstrate for the first time that actin patches form along sensory axons *in situ* and serve as the precursors to the formation of axonal filopodia. Thus, the emergence of filopodia from both axons and dendrites in their natural environment involves the formation of actin patches. Using *in vitro* conditions designed to best match the predicted *in vivo* situation, we find that actin patch formation *in vitro* is remarkably similar to that *in situ*. One major difference between the *in vitro* and *in situ* scenarios is certainly the complement of extracellular matrix and cell adhesion molecules in the immediate environment of the axon. The similarity between the *in vitro* and *in situ* data indicate that *in situ* the axon behaves in a manner similar to in vitro when the axons are growing on laminin. One possibility is that extracellular and cell adhesion molecules may provide permissive, but not instructive, roles for the formation of actin patches which is otherwise governed in large part by cell intrinsic mechanisms. This possibility is suggested by our previous finding that when axons are growing on laminin, in the absence of NGF, actin patches form in the vicinity of clusters of surface integrin receptors but do not directly colocalize with the receptors (Ketschek and Gallo, 2010). However, extracellular matrix molecules and cell adhesion molecules can regulate such fundamental aspects of axon extension as whether axons need actin filaments to extend (Abosch and Lagenaur, 1993). Therefore, in future studies it will be of interest to determine whether different cell adhesion and extracellular matrix molecules regulate the axonal actin patch system. The length of filopodia was shorter in the spinal cord than in vitro. This may reflect the differential activity of extracellular signals in the two situations, or the requirement of filopodia to extend through the surrounding cellular and extracellular environment in the spinal cord which is absent in vitro.

This study determines that the Arp2/3 complex is required for NGF/PI3K-dependent formation of axonal actin patches. PI3K signaling may locally recruit Arp2/3 subunits or regulate the activity of Arp2/3 complex regulators/activators. Consistent with this scenario, we find that the Arp2/3 activator WAVE1 targets to actin patches and WAVE is recruited to the membrane by PIP3 (Takenawa and Suetsugu, 2007). In addition, mRNAs to Arp2/3 complex subunits and cortactin are found in axons (Zivraj et al., 2010), and PI3K activity contributes to the localized translation of some axonal mRNAs in response to NGF (Willis et al., 2007). Additional studies will be required to dissect how the PI3K pathway converges on the Arp2/3 complex.

Multiple actin filament nucleators initiate filaments de novo (i.e., formins, cordon bleu, spire; Pollard, 2007). In contrast, the Arp2/3 complex nucleates new filaments from the sides of existing mother filaments resulting in the formation of branched actin filaments (Pollard et al., 2000). The organization of filaments detected by PREM reveals a complex meshwork of filaments some of which have a geometry consistent with Arp2/3-mediated nucleation. Because the Arp2/3 complex requires mother filaments to nucleate branched filaments, sparse actin filaments normally present in the axonal shafts may serve as mother filaments to support Arp2/3 complex-dependent nucleation in axonal microdomains. Alternatively, additional actin filament nucleators may also operate in actin patches to generate the mother filaments. The nucleation factor cordon-bleu is a likely candidate as it positively contributes to the formation of axon collateral branches and can cooperate with Arp2/3 in the formation of actin filaments (Ahuja et al., 2007).

The axon is a highly polarized structure. The levels and dynamics of actin filaments are greatest at the growth cone while the axon shaft is relatively quiescent. In sensory axons the major actin filament based structures along the axon shaft are actin patches. The current study indicates the presence of opposite gradients in the rates of the initiation of axonal actin patches and their lifespans. These observations unveil a new level of axonal polarization. It will be of interest to further determine the molecular mechanisms underlying patch initiation and lifespan and how these mechanisms are differentially regulated along the axon shaft. In a previous study we found that the gradient in the rate of actin patch initiation in the distal axon was maintained following direct activation of PI3K using PI3Kpep, although the absolute number of actin patches formed per unit time was greatly promoted by PI3Kpep (Ketschek and Gallo, 2010). PI3Kpep treatment increased the lifespan of patches in the distal axon indicating that a distal(high)-proximal(low) gradient of net PI3K activity is unlikely to underlie the observed inverse gradients in the rate of formation and patch lifespan. However, a distal-proximal gradient of PI3K activity may underlie the gradient in the rate of patch formation. Previous studies have indeed determined that the levels of PI3K activity are greatest in the growth cone (Menager et al., 2004; Zhou et al., 2004).

In conclusion, this study determines that the Arp2/3 complex is required for the formation of axonal actin patches and filopodia in sensory neurons downstream of NGF and PI3K signaling. We also provide the first evidence that axonal actin patches are formed *in vivo/in situ* and serve as precursors to the formation of axonal filopodia. The observation that filopodia emerge from only a subset of actin patches suggests that a stochastic mechanism may underlie the triggering of the emergence of a filopodium from a patch. The emergence of filopodia from patches may have a stochastic nature due to the requirement for the convergence of multiple elements of the triggering mechanism within a single patch. Alternatively, sites along the axon where filopodia emerge from patches may be spatially pre-determined, perhaps by membrane targeted mechanism, and thus only patches that form in the appropriate axonal location give rise to filopodia. Future studies will be required to address the mechanism that drives the emergence of filopodia from actin patches. We speculate that proteins known to regulate the reorganization of actin filaments from

branched networks to parallel bundles, such as formins (Yang et al., 2007) and the filament bundling protein fascin (Vignievic et al. 2006), may be operative in patches and drive the emergence of filopodia from patches. Fascin requires dephosphorylation in order to bundle actin filaments, and if operative in patches may thus provide a phosphorylation-based mechanism for the emergence of filopodia from patches (Vignievic et al. 2006). In the context of NGF signaling, the regulation of the initiation of axonal actin patches is the major regulatory point in the NGF-induced increase in the number of axonal filopodia, without a change in the frequency of emergence of filopodia from patches (Ketschek and Gallo, 2010). We suggest that NGF provides a permissive signal to maintain the frequency of the emergence of filopodia from patches at a steady state in conditions of increased rates of actin patch formation (Ketschek et al., 2011).

Supplementary Material

Refer to Web version on PubMed Central for supplementary material.

Acknowledgments

This work was supported by grants to GG (NIH NS 048090), LL (NIH NS 049178) and TS (NIH GM 70898 and RR 22482). We thank Dr. P. Letourneau (U of Minnesota) for assistance with early aspects of the in ovo electroporation work. We also thank Dr. M. Wilson (ECM Biosciences) for providing antibodies to WAVE1 and Arp2. Aspects of Figure 3 are reproduced with permission from John Wiley & Sons, Inc (Developmental Neurobiology, 71(3):201-20).

REFERENCES

Abosch A, Lagenaur C. Sensitivity of neurite outgrowth to microfilament disruption varies with adhesion molecule substrate. J Neurobiol. 1993; 24:344–355. [PubMed: 8492111]

Andersen R, Li Y, Resseguie M, Brenman JE. Calcium/calmodulin-dependent protein kinase II alters structural plasticity and cytoskeletal dynamics in Drosophila. J Neurosci. 2005; 25:8878–8888. [PubMed: 16192377]

Ahuja R, Pinyol R, Reichenbach N, Custer L, Klingensmith J, Kessels MM, Qualmann B. Cordon-bleu is an actin nucleation factor and controls neuronal morphology. Cell. 2007; 131:337–350. [PubMed: 17956734]

Bastmeyer M, O'Leary DD. Dynamics of target recognition by interstitial axon branching along developing cortical axons. J Neurosci. 1996; 16:1450–1459. [PubMed: 8778296]

Cohen-Cory S, Kidane AH, Shirkey NJ, Marshak S. Brain-derived neurotrophic factor and the development of structural neuronal connectivity. Dev Neurobiol. 2010; 70:271–288. [PubMed: 20186709]

Cosker KE, Eickholt BJ. Phosphoinositide 3-kinase signalling events controlling axonal morphogenesis. Biochem Soc Trans. 2007; 35:207–210. [PubMed: 17371239]

Davis BM, Frank E, Johnson FA, Scott SA. Development of central projections of lumbosacral sensory neurons in the chick. J Comp Neurol. 1989; 279:556–566. [PubMed: 2918087]

Drinjakovic J, Jung H, Campbell DS, Strochlic L, Dwivedy A, Holt CE. E3 Ligase Nedd4 Promotes Axon Branching by Downregulating PTEN. Neuron. 2010; 65:341–357. [PubMed: 20159448]

Faix J, Breitsprecher D, Stradal TE, Rottner K. Filopodia: Complex models for simple rods. Int J Biochem Cell Biol. 2009; 41:1656–1664. [PubMed: 19433307]

Gallo G, Letourneau PC. Localized sources of neurotrophins initiate axon collateral sprouting. J Neurosci. 1998; 18:5403–5414. [PubMed: 9651222]

Gallo G, Letourneau PC. Different contributions of microtubule dynamics and transport to the growth of axons and collateral sprouts. J Neurosci. 1999; 19:3860–3873. [PubMed: 10234018]

Gallo G. RhoA-kinase coordinates F-actin organization and myosin II activity during semaphorin-3A-induced axon retraction. J Cell Sci. 2006; 119:3413–3423. [PubMed: 16899819]

Gallo G. The cytoskeletal and signaling mechanisms of axon collateral branching. Dev Neurobiol. 2011; 71(3):201–220. [PubMed: 21308993]

Gan WB. Glutamate-dependent stabilization of presynaptic terminals. Neuron. 2003; 38:677–678. [PubMed: 12797951]

Gibson DA, Ma L. Developmental regulation of axon branching in the vertebrate nervous system. Development. 2011; 138(2):183–195. [PubMed: 21177340]

Halloran MC, Kalil K. Dynamic behaviors of growth cones extending in the corpus callosum of living cortical brain slices observed with video microscopy. J Neurosci. 1994; 14:2161–2177. [PubMed: 8158263]

Kalil K, Szebenyi G, Dent EW. Common mechanisms underlying growth cone guidance and axon branching. J Neurobiol. 2000; 44:145–158. [PubMed: 10934318]

Ketschek A, Gallo G. Nerve growth factor induces axonal filopodia through localized microdomains of phosphoinositide 3-kinase activity that drive the formation of cytoskeletal precursors to filopodia. J Neurosci. 2010; 30:12185–12197. [PubMed: 20826681]

Ketschek A, Spillane M, Gallo G. Mechanism of NGF-induced formation of axonal filopodia: NGF turns up the volume, but the song remains the same? Communicative and Integrative Biol. 2011; 4(1):55–58.

Korobova F, Svitkina T. Arp2/3 complex is important for filopodia formation, growth cone motility, and neuritogenesis in neuronal cells. Mol Biol Cell. 2008; 19:1561–1574. [PubMed: 18256280]

Kwon CH, Luikart BW, Powell CM, Zhou J, Matheny SA, Zhang W, Li Y, Baker SJ, Parada LF. Pten regulates neuronal arborization and social interaction in mice. Neuron. 2006; 50:377–388. [PubMed: 16675393]

Letourneau PC. Actin in axons: stable scaffolds and dynamic filaments. Results Probl Cell Differ. 2009; 48:65–90. [PubMed: 19582412]

Loudon RP, Silver LD, Yee HF Jr, Gallo G. RhoA-kinase and myosin II are required for the maintenance of growth cone polarity and guidance by nerve growth factor. J Neurobiol. 2006; 66:847–867. [PubMed: 16673385]

Lundquist EA. The finer points of filopodia. PLoS Biol. 2009; 7(6):e1000142. [PubMed: 19564901]

Mattila PK, Lappalainen P. Filopodia: molecular architecture and cellular functions. Nat Rev Mol Cell Biol. 2008; 9:446–454. [PubMed: 18464790]

Ménager C, Arimura N, Fukata Y, Kaibuchi K. PIP3 is involved in neuronal polarization and axon formation. J Neurochem. 2004; 89:109–118. [PubMed: 15030394]

Mendelson B, Koerber HR, Frank E. Development of cutaneous and proprioceptive afferent projections in the chick spinal cord. Neurosci Lett. 1992; 138:72–76. [PubMed: 1383880]

Mingorance-Le Meur A, O'Connor TP. Neurite consolidation is an active process requiring constant repression of protrusive activity. EMBO J. 2009; 28:248–260. [PubMed: 19096364]

Nolen BJ, Tomasevic N, Russell A, Pierce DW, Jia Z, McCormick CD, Hartman J, Sakowicz R, Pollard TD. Characterization of two classes of small molecule inhibitors of Arp2/3 complex. Nature. 2009; 460:1031–1044. [PubMed: 19648907]

Norris AD, Dyer JO, Lundquist EA. The Arp2/3 complex, UNC-115/abLIM, and UNC-34/Enabled regulate axon guidance and growth cone filopodia formation in Caenorhabditis elegans. Neural Dev. 2009; 4:38. [PubMed: 19799769]

Orlova I, Silver L, Gallo G. Regulation of actomyosin contractility by PI3K in sensory axons. Dev Neurobiol. 2007; 67:1843–1851. [PubMed: 17701990]

Patel TD, Jackman A, Rice FL, Kucera J, Snider WD. Development of sensory neurons in the absence of NGF/TrkA signaling *in vivo*. Neuron. 2000; 25:345–357. [PubMed: 10719890]

Petruska JC, Mendell LM. The many functions of nerve growth factor: multiple actions on nociceptors. Neurosci Lett. 2004; 361:168–171. [PubMed: 15135920]

Pollard TD. Regulation of actin filament assembly by Arp2/3 complex and formins. Annu Rev Biophys Biomol Struct. 2007; 36:451–477. [PubMed: 17477841]

Pollard TD, Blanchoin L, Mullins RD. Molecular mechanisms controlling actin filament dynamics in nonmuscle cells. Annu Rev Biophys Biomol Struct. 2000:545–576. [PubMed: 10940259]

Portera-Cailliau C, Weimer RM, De Paola V, Caroni P, Svoboda K. Diverse modes of axon elaboration in the developing neocortex. PLoS Biol. 2005; 3(8):e272. [PubMed: 16026180]

Silver L, Qiang L, Loudon R, Gallo G. Bidirectional inhibitory interactions between the embryonic chicken metanephros and lumbosacral nerves *in vitro*. Dev Dyn. 2004; 231(1):190–198. [PubMed: 15305299]

Strasser GA, Rahim NA, VanderWaal KE, Gertler FB, Lanier LM. Arp2/3 is a negative regulator of growth cone translocation. Neuron. 2004; 43:81–94. [PubMed: 15233919]

Svitkina TM, Bulanova EA, Chaga OY, Vignjevic DM, Kojima S, Vasiliev JM, Borisy GG. Mechanism of filopodia initiation by reorganization of a dendritic network. J Cell Biol. 2003; 160:409–421. [PubMed: 12566431]

Svitkina T. Imaging cytoskeleton components by electron microscopy. Methods Mol Biol. 2009; 586:187–206. [PubMed: 19768431]

Takenawa T, Suetsugu S. The WASP-WAVE protein network: connecting the membrane to the cytoskeleton. Nat Rev Mol Cell Biol. 2007 Jan; 8(1):37–48. [PubMed: 17183359]

Vignjevic D, Kojima S, Aratyn Y, Danciu O, Svitkina T, Borisy GG. Role of fascin in filopodial protrusion. J Cell Biol. 2006; 174:863–875. [PubMed: 16966425]

Williams EJ, Doherty P. Evidence for and against a pivotal role of PI 3-kinase in a neuronal cell survival pathway. Mol Cell Neurosci. 1999; 13(4):272–280. [PubMed: 10328886]

Willis DE, van Niekerk EA, Sasaki Y, Mesngon M, Merianda TT, Williams GG, Kendall M, Smith DS, Bassell GJ, Twiss JL. Extracellular stimuli specifically regulate localized levels of individual neuronal mRNAs. J Cell Biol. 2007; 178:965–980. [PubMed: 17785519]

Yang C, Czech L, Gerboth S, Kojima S, Scita G, Svitkina T. Novel roles of formin mDia2 in lamellipodia and filopodia formation in motile cells. PLoS Biol. 2007; 5:e317. [PubMed: 18044991]

Zhou FQ, Zhou J, Dedhar S, Wu YH, Snider WD. NGF-induced axon growth is mediated by localized inactivation of GSK-3beta and functions of the microtubule plus end binding protein APC. Neuron. 2004; 42:897–912. [PubMed: 15207235]

Zivraj KH, Tung YC, Piper M, Gumy L, Fawcett JW, Yeo GS, Holt CE. Subcellular profiling reveals distinct and developmentally regulated repertoire of growth cone mRNAs. J Neurosci. 2010; 30:15464–15478. [PubMed: 21084603]

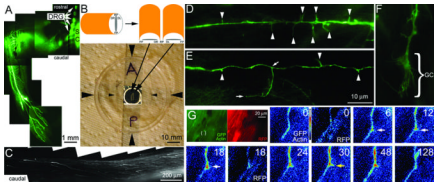

FIGURE 1. Acute *ex vivo* spinal cord model

(A) Example of the ventral portion of the hind limb of an ED 9 embryo whole mount transfected with GFP at day 3. The image is a montage of 4× images. Transfected DRGs are readily detected (arrows) as are transfected cells in a few segments of the spinal cord (SC). GFP labeled nerves are detectable throughout the limb. **(B)** The schematic shows the orientation of the bisected cord when placed on the glass coverslip of the chamber system. The photograph shows the assembled chamber system. Large arrowheads denote the sides of the chamber. The small arrowheads denote the sides of the coverslip laid on top of the well in the chamber forming a sealed environment. The well in the center of the dish is contrast enhanced. Resting within the well is a bisected spinal cord as shown in the schematic. A=anterior/rostral, P=posterior/caudal. **(C)** Example of GFP-labeled DRG axons extending in the caudal dorsal funniculi of an explanted spinal cord. The image is a montage of 20× images. Note the absence of other GFP-transfected cells. **(D)** Example of axonal filopodia (arrowheads) extending from a GFP-transfected axon (100×). **(E)** Example of axonal filopodia and a branch approximately 18 μm in length (100×). The base and tip of the branch are denoted by arrows. **(F)** Example of a growth cone (GC; 100×; also see Figure 4E). **(G)** The green and red panels show the 100× imaging field for the GFP-actin and RFP channels respectively. The area of interest shown in the false colored panels is denoted by brackets. The timelapse sequence shows the GFP-actin and RFP channels representing a co-transfected axon. Time is in seconds. An actin patch forms at 6 sec, gives rise to a filopodium at 30 sec (yellow arrow) and dissipates by 128 sec. The RFP channel (0 and 18 sec) does not reveal a similar localized increase in fluorescence.

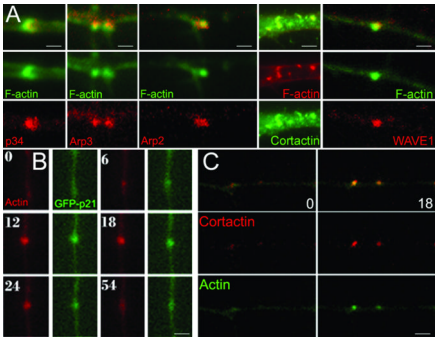

Figure 2. Localization of the Arp2/3 complex to actin patches

(A) Immunocytochemical localization of Arp2/3 subunits, cortactin and WAVE1 to axonal actin patches along axons *in vitro*. Differences in the size of patches in fixed samples represent patches being at different points during their lifespan at the time of fixation. **(B)** Timelapse sequence (seconds) of axon cotransfected with the GFP-p21 Arp2/3 complex subunit and mCherry-actin. **(C)** As in (B) but showing RFP-cortactin and eYFP-actin. (B) and (C) are from *in vitro* studies. Bars = 1 μm.

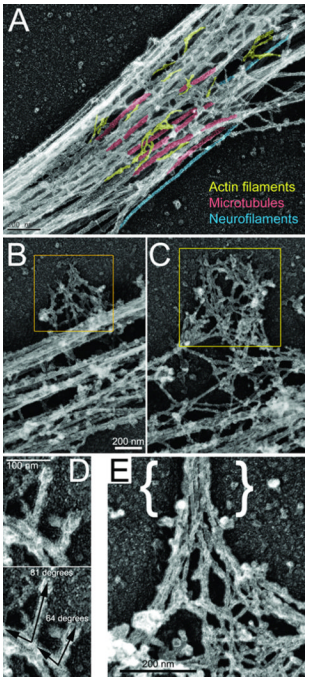

Figure 3. Organization of the axonal cytoskeleton revealed by PREM

(A) Representative axonal shaft showing abundant microtubules (red), sparse actin filaments (yellow), and occasional intermediate filaments (blue). **(B, C)** Examples of lateral patches of the axonal actin network (yellow boxes; bar in B also applies to C). **(D)** Actin filament bundle in the axonal filopodium ({}) emerging from a network in the lateral patch. **(E)** Examples of branched filaments observed in lateral patches. Angle measurements for each branch is shown in bottom panel. (A,C) This material is reproduced with permission of John Wiley & Sons, Inc (Gallo, 2011).

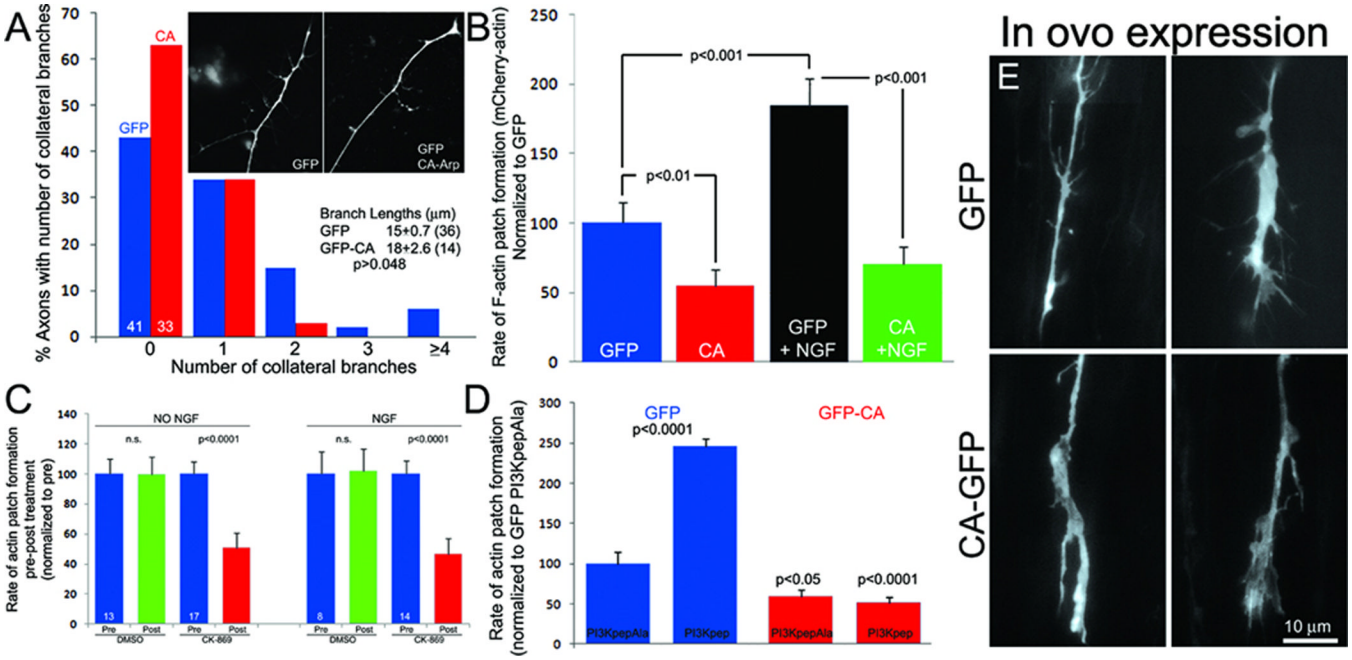

Figure 4. The Arp2/3 complex contributes to the formation of actin patches, filopodia and branches

(A) Transfection with GFP-CA decreased the numbers of axon collateral branches sampled from the distal 100 µm of axons *in vitro* (Mann Whitney, p=0.025; inset shows representative axonal morphology). Numbers of scored axons are shown within respective bars. **(B)** Rate of actin patch formation in GFP-CA-expressing neurons relative to GFP control with or without a 30 min treatment with NGF (Welch t-test, n≥15 axons/group). **(C)** The rate of actin patch formation before and after a 10 min treatment with CK-869 or DMSO in the absence and presence of NGF. **(D)** The rate of actin patch formation in the absence of NGF after treatment with PI3Kpep relative to treatment with control PI3KpepAla peptide in neurons expressing GFP (blue) or GFP-CA (red). n≥15 axons/group. **(E)** Examples of in ovo transfected GFP and GFP-CA expressing distal axons in the *ex vivo* spinal cord.

TABLE I

Comparison of actin patch dynamics detected through fluorescently labeled actin and the length of filopodia *in vitro* relative to in the living spinal cord

	in vitro	**in the spinal cord**	**p value**
Rate of patch formation (patches/20 /μm/5 min)	2.04±0.4 (9)	2.08±N/A[a] (10)	N/A
Patch lifespan (sec)	48±4.6 (71)	41.4±1.8 (52)	p=0.16*
Probability of emergence of filopodia (0–1)	0.15 (71)	0.17 (52)	p=0.8**
Patch size (pixels^2)	22 (36)	23 (30)	p=0.3***
Length of filopodia (μm)	3.6 (73)	2.9 (146)	p<0.01***

Mean+SEM (n) are shown for the rate and lifespan data.

[a] SEM is not available for the rate of patch formation in the spinal cord due to the sampling method, see main text. Patch sizes and filopodial lengths were not normally distributed and the median (n) is shown.

* Welch t-test,

** X^2 test,

*** Mann-Whitney test.